

# Partitioning of intermontane basins by thrust-related folding, Tien Shan, Kyrgyzstan

D. W. Burbank,\* J. K. McLean,† M. Bullen,\* K. Y. Abdrakhmatov‡ and M. M. Miller†

\*Department of Geosciences, Pennsylvania State University, University Park, PA 16802, USA

†Department of Geology, Central Washington University, Ellensburg, WA 98926, USA

‡Institute of Seismology, Bishkek, Kyrgyzstan

## ABSTRACT

Well-preserved, actively deforming folds in the Tien Shan of Kyrgyzstan provide a natural laboratory for the study of the evolution of thrust-related folds. The uplifted limbs of these folds comprise weakly indurated Cenozoic strata that mantle well-lithified Palaeozoic bedrock. Their contact is a regionally extensive unconformity that provides a persistent and readily traceable marker horizon. Based on the deformation of this marker, preserved fold geometries support simple geometric models for along-strike gradients in fold amplitude and displacement along the underlying faults, linkage among multiple structures, transfer of displacement among folds and evolution of the folds as geomorphic entities. Subsequent to initial uplift and warping of the unconformity surface, steeply dipping reverse faults cut the forelimbs of many of these folds. Wind gaps, water gaps, recent faulting and progressive stripping of the more readily eroded Cenozoic strata indicate the ongoing lateral propagation and vertical growth of fault-related folds. The defeat of formerly antecedent rivers coincides in several places with marked increases in erosional resistance where their incising channels first encountered Palaeozoic bedrock. Persistent dip angles on the backlimbs of folds indicate strikingly uniform geometries of the underlying faults as they propagate both laterally and vertically through the crust. Deformation switches irregularly forward and backward in both time and space among multiple active faults and folds with no systematic pattern to the migration of deformation. This distributed deformation appears characteristic of the entire Kyrgyz Tien Shan.

## INTRODUCTION

Intracontinental mountain building in convergent settings usually occurs as a result of the nucleation and growth of thrust faults. As thrust belts emerge as topographic entities, they define intermontane basins in which the detritus eroded from the bounding ranges accumulates. As convergence continues, at least three patterns of deformation can accommodate the ongoing shortening: the early formed thrusts can continue to move and accumulate more and more displacement; the zone of deformation can widen as new thrusts emerge along the flanks of the mountain belt; or new thrusts can develop within and between the existing mountains during densification of the thrust system. In this last scenario, the new thrusts will often encroach upon or subdivide the pre-existing intermontane basins.

The Tien Shan of Kyrgyzstan represent a zone of intracontinental convergence in which shortening occurs in response to the ongoing convergence between India and Siberia. Recent geodetic studies indicate present

shortening rates of  $\approx 13 \text{ mm yr}^{-1}$  within the Kyrgyz Tien Shan (Abdrakhmatov *et al.*, 1996) and suggest that, when the shortening along the northern margin of the Tarim Basin is included, the total shortening is likely to be  $\approx 20 \text{ mm yr}^{-1}$  (Michel *et al.*, 1997): an amount equal to  $\approx 40\%$  of the modern Indo-Asian convergence rate. In western Kyrgyzstan, the Tien Shan comprises five thrust-bounded ranges which are aligned approximately east–west and are separated from each other by intermontane basins typically 15–50 km wide (Chediya, 1986; Ghose *et al.*, 1996) (Fig. 1). Whereas shortening is presently occurring along existing range-bounding thrusts and the overall zone of deformation appears to be widening to the north (the first two options above), it is clear that the present intermontane basins are also being partitioned by the development of new thrust faults.

In the southern Naryn Basin and directly to the south of the Naryn River, an array of thrusts and fault-related folds have emerged which define the current basin margin (Fig. 2) and which separate the Naryn Basin from the At Bashi basin to the south (Omuraliev & Korzhenkov,

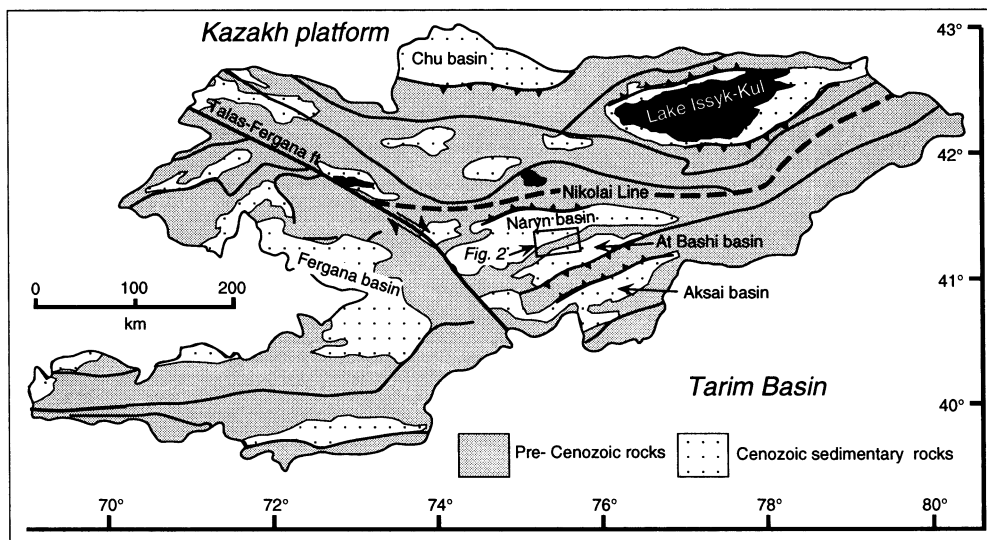


Fig. 1. Schematic map of the major ranges and basins of the Tien Shan in the Kyrgyz Republic. Study area encompasses the ranges which define the present-day southern margin of the Naryn Basin and northern margin of the At Bashi Basin. Modified after Geological map of Kirghiz SSR (1980).

1995). These structures range from nascent folds to strongly emergent bedrock folds which are cut by steeply dipping reverse faults and which exhibit as much as 7 km of structural relief. The resultant ranges provide an excellent opportunity to examine the growth of fault-related folds, displacement transfer between multiple structures, spatial and temporal displacement variations, and the geomorphic response to rock uplift within these active folds and thrusts. In this paper, we present simple models which relate the growth of individual and multiple structures with geomorphic processes. Based on reconnaissance mapping, field observations, and interpretation of satellite images and aerial photography, we examine the ranges bounding the southern Naryn Basin in the context of the models. Finally, we discuss what the structures and geomorphology suggest in terms of the sequence of deformation and the way in which the upper crust responds to continued contractional stresses.

## BACKGROUND GEOLOGY OF THE TIEN SHAN

The Tien Shan of Kyrgyzstan are bounded by the Tarim Basin to the south and the relatively stable Kazakh platform to the north. Comprising primarily Palaeozoic rocks and lesser amounts of lower Mesozoic strata (USSR, ANKSaMoG, 1980), the Tien Shan were deformed by two Palaeozoic orogenies (Burtman, 1975). The approximately east-west-trending 'Nikolai Line' in the central Tien Shan (Fig. 1) defines a tectonic boundary in central Kyrgyzstan between extensively intruded rocks to the north that were deformed in early Palaeozoic times and unintruded strata to the south that were deformed during late Palaeozoic times (Burtman, 1975). Lying south of the Nikolai Line, the bedrock ranges of the

southern Naryn Basin comprise Palaeozoic miogeoclinal strata, primarily Carboniferous carbonate and siliciclastic strata. Following Palaeozoic and early to mid Mesozoic deformation, the bedrock throughout the study area was largely bevelled by erosion prior to the onset of extensive Cenozoic deposition (Makarov, 1977; Sadybakasov, 1990).

The profound, commonly angular, unconformity across the pre-Cenozoic rocks provides a remarkable structural marker that can be used to define the magnitude of folding and rock uplift within many parts of the Tien Shan (Chediya, 1986; Omuraliev & Korzhenkov, 1995). During the early Cenozoic in the study area, the tilt and topographic relief on this unconformity appear to have been minimal. Prominently bedded Cenozoic strata overlying the Palaeozoic bedrock can be traced extensively along the flanks of folds in the study area. Because the stratigraphic height of nearly any traceable Cenozoic bed above the unconformity varies by less than a few metres across the several kilometres of these exposures, it is clear that the unconformity can be considered to be a nearly horizontal datum at the time of initial Cenozoic deposition. Thus, subsequent tilting, uplift, folding and faulting of this surface provide key controls on the magnitude of Cenozoic deformation.

Palaeontological studies indicate that Cenozoic strata in the Naryn and At Bashi basins span from Oligocene to Quaternary times (Turbin *et al.*, 1972). These strata are nonmarine and comprise facies associations interpreted to represent alluvial fan, fluvial, floodplain and shallow lacustrine depositional settings. In the study area, the Cenozoic strata prior to deformation were generally 4–6 km thick (Makarov, 1977; Sadybakasov, 1990). These strata are weakly to moderately cemented and are far more readily eroded than the underlying Palaeozoic rocks.

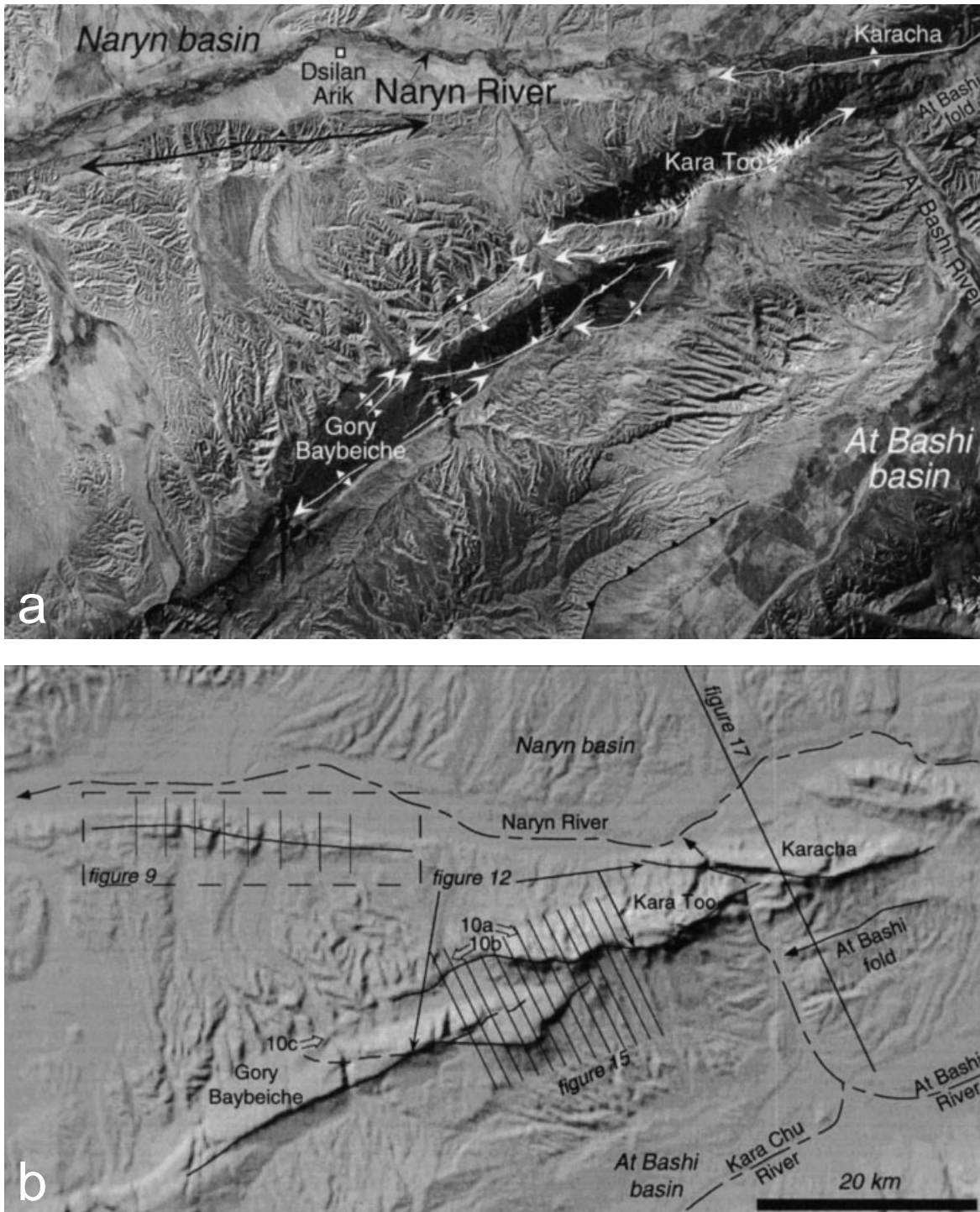


**Fig. 2.** a. Satellite image of the southern Naryn Basin and the bedrock uplifts that separate it from the At Bashi Basin. Schematic structures are also depicted. The highly dissected parts of the landscape correspond with Cenozoic strata, whereas the smooth surfaces along the northern flank of the major uplifts represent the uplifted, exposed, but little dissected unconformity surface cut across Palaeozoic bedrock. b. Smoothed topography of the study area and location of subsequent figures. For location, see Fig. 1.

## MODELS FOR FAULT AND FOLD GROWTH AND GEOMORPHIC INTERACTIONS WITH GROWING FOLDS

### Growth and linkage of individual thrust faults and folds

Both thrust and normal faults appear to follow similar scaling laws for growth (Boyer & Elliott, 1982; Dawers *et al.*, 1993; Scholz *et al.*, 1993; Anders & Schleische, 1994; Cartwright *et al.*, 1995; Clark & Cox, 1996), in that, as displacement accumulates, the faults propagate laterally and lengthen (Cowie & Scholz, 1992a). Displacement gradients along individual faults display a bow-like or bell-shaped geometry (Elliott, 1976; Cowie & Scholz, 1992b) with a rapid tapering of displacement toward the tips (Fig. 3). The ratio of maximum displacement to fault length for thrusts tends to vary from 1:10 to 1:100 (Scholz, 1990). As with normal faults (Cartwright *et al.*, 1995; Dawers & Anders, 1995), thrust faults may develop as isolated structures, or may link up with adjoining thrusts as propagating thrust tips interfere with and intersect each other (Fig. 3). Although linkage among multiple thrusts gradually smooths variations in displacement gradients, zones of lesser displacement (deficits) along strike may mark the location of overlap and joining of formerly separate thrusts in a style similar to that proposed for normal faults (Simpson & Anders, 1992; Anders & Schleische, 1994).

Deformation patterns of fold limbs developed above

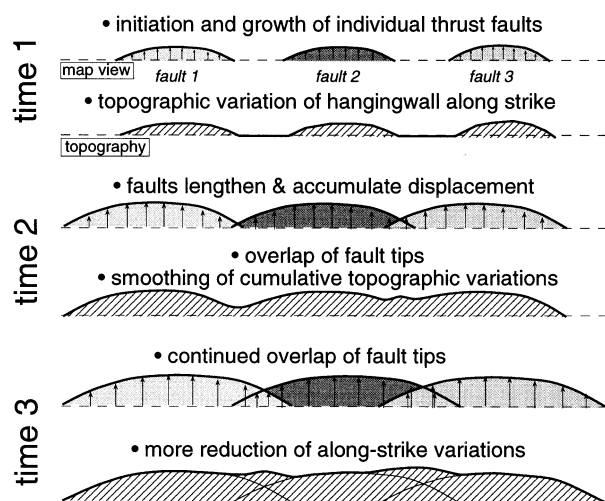


Fig. 3. Thrust faults growing as individual structures and linking during thrust-tip propagation. When examined in isolation, displacement and topography of the uneroded hangingwall varies strongly both along individual thrusts (note the bow- or bell-shaped displacement gradients) and along strike among several thrusts. As these thrusts begin to overlap and join into a single thrust surface, the variations in displacement and topography gradually smooth along strike. Where several thrusts have merged along strike, displacement deficits can indicate the zones of linkage between two adjacent thrusts.

blind thrusts depend on the fault slip-to-propagation ratio, the geometry of the underlying faults, the mechanical behaviour of the deforming strata and the geometry of folding. For example, folds that develop via fault propagation, buckle, detachment, displacement gradient or trishear each have different predicted deformational geometries (Suppe & Medwedeff, 1990; Erslev, 1991; Homza & Wallace, 1995; Allmendinger, 1998). Because of these differences in fold geometries, there is no guarantee that crestal uplift in a fold is linearly related to displacement on the underlying fault. Nonetheless, if a given style of deformation persists along strike, then there may be a consistent and predictable relationship between fold growth and increasing displacement on the causative faults. In such cases, the amplitude of folding as exemplified by the structural relief on the fold crest provides a proxy for displacement on the underlying faults.

### Transfer of displacement among multiple folds

In *en echelon* structures, the propagating tips of faults often do not physically link together as the faults grow. Although the trends of the fault surfaces are parallel to one another, they are offset from each other perpendicular to strike (Philip & Meghraoui, 1983; Sylvester, 1988; Davis *et al.*, 1989; Dawers & Anders, 1995). In these circumstances, as the displacement along one fault dies towards its tip, this decrease may be compensated for by increasing offset on an *en echelon* fault. When folds develop above *en echelon* blind thrusts, the magnitude of shortening, as reflected by the amplitude of folding, may display similar compensation among parallel, but offset structures (Fig. 4). Any individual thrust fault or fold will commonly reveal strong gradients in displacement or in amplitude along the structure. When regional shortening is integrated perpendicular to strike through multiple overlapping structures, however, variations in total displacement may be considerably smoothed. This should be the expected condition if shortening is occurring within a zone bounded by two rigid, converging crustal blocks and is accommodated by an array of structures developing along their common boundary. Such a condition would indicate that stresses are uniformly distributed throughout the region. In the case of multiple folds, transfer of displacement between structures can be inferred from comparisons of bed-length changes along those parts of the folds that overlap in an orientation perpendicular to the regional shortening direction (Fig. 4).

### Geomorphic evolution of folds

As folding and thrusting propagate into a depositional basin, the growing structures convert regions that were formerly depositional basins into erosional source areas.

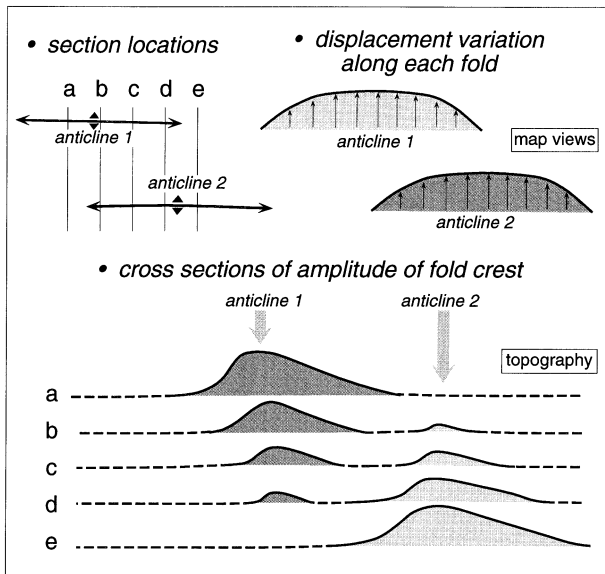


Fig. 4. Transfer of displacement among two *en echelon* folds. As displacement decreases toward the nose of one fold, it increases in the adjacent fold. Shortening recorded by bed-length changes in each fold shows displacement compensation which smoothes the integrated displacement variation between the two folds.

The emergent crest of the fold will be a plunging structure that propagates laterally as the underlying fault accumulates displacement. Typically the emergent fold comprises weakly lithified, recently deposited sediment that can be readily eroded. When catchment areas on the rising fold are large enough to provide a sufficient water discharge and when slopes are adequately steep, channels are incised into the formerly pristine fold surface (Dietrich *et al.*, 1992; Montgomery & Dietrich, 1992). Through time as the fold limbs grow, these channels expand to cover the flanks of the fold and are driven headward into the bedrock. Stream density, dissection of the fold surface, sediment flux, and mass-wasting into channel heads and flanks all tend to increase as the fold is amplified (Brozovic *et al.*, 1995; Burbank *et al.*, 1996c; Talling *et al.*, 1997; Keller *et al.*, 1998). If the pregrowth strata, i.e. those strata deposited prior to the initiation of fold growth (Suppe *et al.*, 1992), are lithologically uniform, predictable geomorphic changes develop along the length of the plunging, growing fold.

Our model for fold evolution in the Tien Shan resembles the general model described above, with two important exceptions: first, the forelimbs of many of the folds are cut by high-angle reverse faults that contribute to crestal uplift, but also interrupt the smooth fold geometry; and second, the marked contrast in erodability between the Cenozoic and Palaeozoic rocks strongly influences the large-scale geomorphic shape of the fold (Fig. 5). As a fold initiates and its crest is raised above local base level, ready incision and stripping of the weakly cemented Cenozoic strata results in a high drainage density on its limbs. As shortening and crestal uplift

continue, Palaeozoic rocks may also be carried above local base level and subjected to erosion. Because it requires greater erosive energy to initiate channel incision in the Palaeozoic strata, stripping of the Cenozoic strata initially reveals the folded, but largely undissected erosion surface. Owing to the higher threshold for channel initiation in the Palaeozoic rocks, the drainage density that is eventually etched into the unconformity surface is much lower than that found in the Cenozoic strata. Once the Cenozoic strata are removed, a key attribute of many of these folds is the persistence of the unconformity surface whose geometry helps define both the magnitude of shortening and the geometry of the subsurface deformation (Omuraliev & Korzhnikov, 1995).

The relative geomorphic age of the fold can be inferred from the amount of structural uplift of rocks in the fold, the degree of stripping of the weaker strata from the crest and flanks of the fold and the degree of preservation or erosion of the unconformity surface bounding the Palaeozoic rocks. Geomorphically older, larger folds are characterized by more removal of Cenozoic strata from their crest and flanks, by increasing dissection of the resistant Palaeozoic rocks and by gradual erosional obliteration of the unconformity surface that defines the shape of the fold.

The growth of a fold as a topographic feature causes interactions with the pre-existing drainage network. In general, antecedent rivers that cross the axes of growing folds (Fig. 6) can either maintain their courses across the fold or be deflected away from its rising crest (Oberlander, 1985; Burbank *et al.*, 1996c; Tucker & Slingerland, 1996). Persistence of an antecedent river across a fold is favoured by slow rates of rock uplift in the fold, readily eroded strata across the fold crest and rivers with large upstream catchments and high discharges. Deflection is promoted by rapid rates of fold growth, crestal rocks that are resistant to erosion and low discharge in the rivers whose former courses traversed the fold axis. In circumstances where erodable strata lie above resistant strata, antecedent rivers are likely to persist across growing folds until they encounter resistant strata, at which point some rivers, especially those with low discharge, may be defeated and deflected (Fig. 6).

In order to maintain an antecedent course, a river must incise over time approximately as rapidly as rock uplift occurs in the crestal area of the fold. For most folds growing above blind faults, coseismic fold growth greatly outpaces river incision (Meghraoui *et al.*, 1988). If, however, the interseismic interval is sufficiently long, if interseismic rock uplift is sufficiently small and if the river is sufficiently powerful, river incision can keep pace with the long-term rock-uplift rates (Burbank *et al.*, 1996b). Although there is no single mechanistic explanation that is widely accepted for erosion by rivers (Slingerland *et al.*, 1998), one commonly cited measure of a river's ability to incise its bed is its unit stream power (Howard *et al.*, 1994): the energy that is available to do work on a given area of the river bed (Fig. 7). An

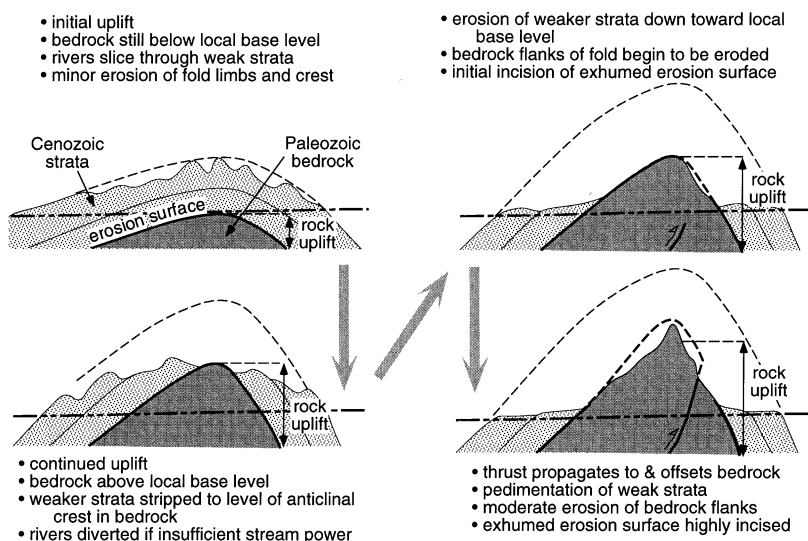


**Fig. 5.** Structural and geomorphic development of a fold. Strong contrasts in erodability favour rapid removal of the overlying, weakly cemented strata, whereas the well-lithified Palaeozoic rocks resist erosion. The unconformity between these strata provides a reliable marker with which to track the deformation. With sufficient rock uplift, the bedrock also begins to be significantly modified by erosion.

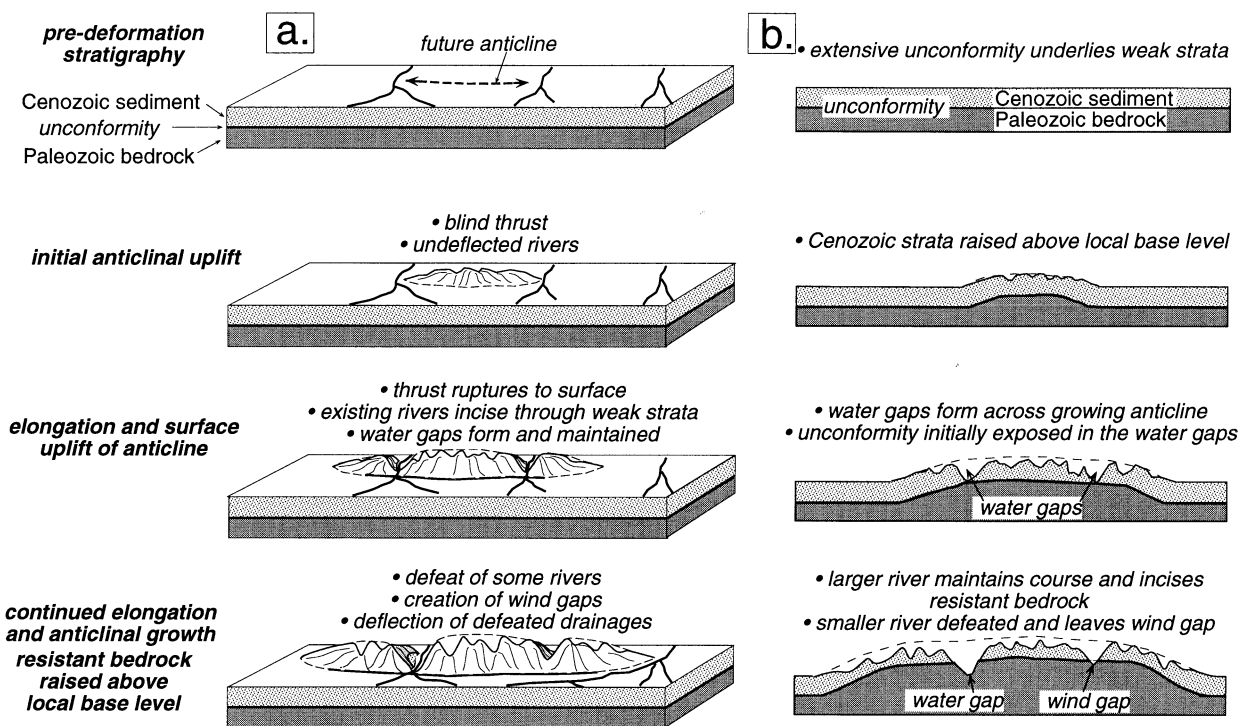


**Fig. 6.** Interactions of folds with rivers. a. Perspective view of a growing fold with two antecedent rivers traversing the fold trend. The strata within the fold comprise a succession of weakly resistant strata underlain by highly resistant strata. As the fold lengthens and its crest rises, rivers initially maintain their courses because they readily incise the weak strata. When more resistant strata are encountered, the stream with the lesser stream power is defeated and then deflected around the nose of the fold. This defeat creates a wind gap that marks the former position of the antecedent river. b. Cross-sectional view of the fold shows ready incision into weak strata, followed by defeat of one formerly antecedent stream when resistant rocks are encountered and local stream power is insufficient to maintain the river's course across the fold.

erosion rate based on unit stream power would be proportional to  $(Q \cdot S)/w$ , where  $Q$  = discharge,  $S$  = river slope and  $w$  = river width. Because discharge is proportional to upstream catchment area (Howard *et al.*, 1994), river erosion rates will be enhanced by any combination of large catchments, steep river gradients and narrow river widths (Fig. 7).

## TECTONIC GEOMORPHOLOGY OF THE SOUTHERN NARYN BASIN

### Growth of individual and linked folds

Two types of folds are apparent in the southern Naryn Basin: nascent folds that have lifted only Cenozoic strata above local base level and more fully developed folds

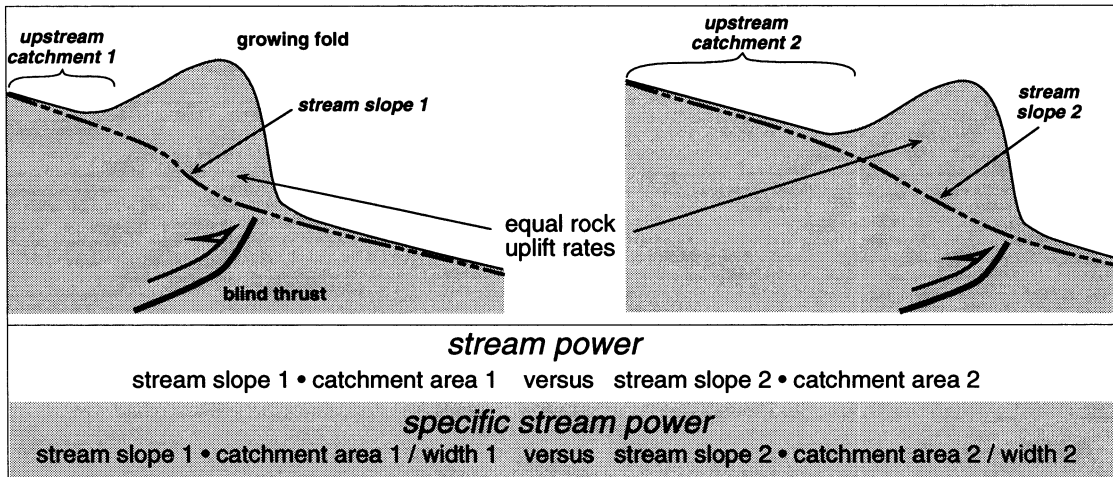


Fig. 7. Schematic relationships between discharge, stream slope and channel width for antecedent streams traversing a rising anticline. Discharge is assumed to be proportional to upstream catchment area. Steep river gradients and large upstream catchments increase total stream power. For any given discharge and slope, specific stream power increases with decreasing river width. The greater the specific stream power, the more rapidly the river is able to incise the bedrock of its bed and the more likely it will be able to keep pace with rock uplift in a fold.

that carry Palaeozoic rocks above local base level (Fig. 8). A clear example of the former type is found parallel to and just south of the Naryn River at Dsilan Arik (Figs 2a and 9). The topographic crest of this fold sits only 400 m above the surrounding plains. The opposing noses of the fold plunge symmetrically at  $\approx 3\text{--}4^\circ$ . When the topographic discontinuities at the water and wind gaps are ignored, the crestal profile displays a broad, bell-shaped profile (Figs 3 and 9).

Several closely spaced antecedent rivers traverse the fold axis, their gradients through the water gaps are typical for small rivers in active folds ( $0.5\text{--}2^\circ$ ) (Burbank *et al.*, 1996) and some of their catchments extend only a few kilometres into the hinterland. One stream has been

defeated and its former course is represented by a wind gap (Fig. 9b). The channels which led to this former water gap are clearly preserved in the upstream alluvial surface (Fig. 9a).

These observations are interpreted to indicate that only modest unit stream power is required to incise river beds fast enough to keep pace with the rising strata. Preservation of the channels upstream of the wind gap suggests that abandonment only occurred recently. As might be predicted, the smallest stream traversing the crest of the fold was defeated first. Overall, this fold is interpreted to typify these characteristics of the early stages of the growth and geomorphic evolution of folds in this area: structural uplift of only a few hundred

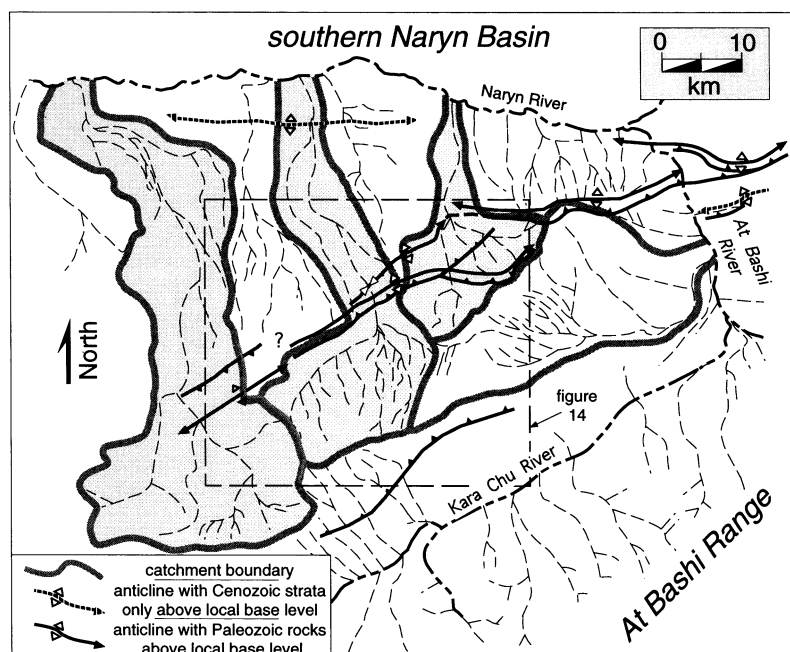


Fig. 8. Drainage map of the southern Naryn and western At Bashi basins, showing the location and orientation of major structures. There are three categories of catchment areas with respect to structure. Those traversing across growing folds are shown in grey. Other catchments are restricted to either the forelimb (south side) or backlimb (north side) of the major folds.

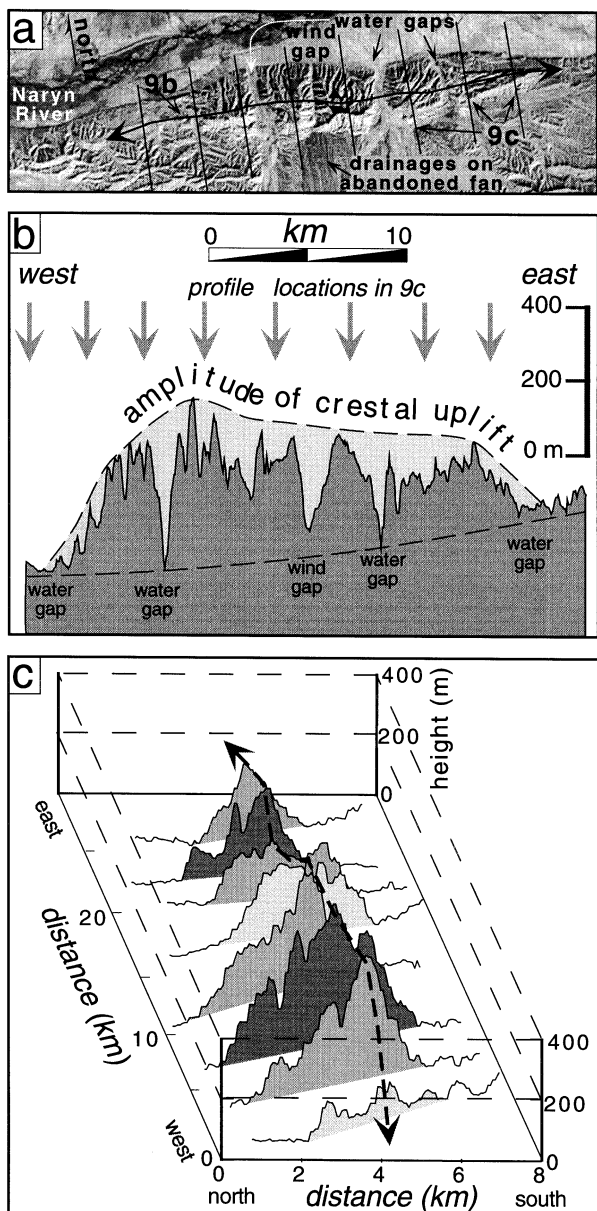


Fig. 9. a. Young, growing fold on the south side of the Naryn River (see Fig. 2b for location). The surface of the fold has been modified by fluvial erosion on both flanks. Antecedent rivers cut through the fold in several locations. Only one major wind gap has developed and defeat of the antecedent river there is recent as evidenced by the clear upstream channels leading to the present wind gap. b. Despite considerable dissection of the uplifted Cenozoic strata, a topographic profile along strike illustrates the bow-shaped, smoothly varying amplitude of crestal uplift along the fold axis and the positions of the water and wind gaps along its length. c. Across-strike profiles depict the widening of the fold as it gains displacement, but reveal little about the internal fold geometry.

metres, ready incision by antecedent rivers, a high density of small streams developed in Cenozoic strata on the fold flanks and considerable modification of the fold shape due to dissection of poorly indurated strata (Figs 5 and 9). As shortening and crestal uplift continue in the southern Naryn Basin, greater thicknesses of Cenozoic strata

and eventually Palaeozoic bedrock are raised above local base level. As much as 5 km of fold amplification may be required, however, before Palaeozoic rocks are raised above local base level. Although the Cenozoic strata tend to be stripped rapidly from the crest and flanks of the fold, several hundred metres to several kilometres of strata may arch across the fold crest in the early stages of fold amplification. In any folds in which the Palaeozoic bedrock has been raised more than  $\approx 500$  m above the adjacent valleys, the Cenozoic strata have been entirely removed from the crest and upper limbs of the fold. Folds which have experienced several kilometres of rock uplift preserve hogbacks or flatirons of Cenozoic strata only along the lower few hundred metres of their flanks (Fig. 10). On all of the large folds studied in the southern Naryn Basin, the unconformity at the base of the Cenozoic strata is extensively preserved across their flanks (Fig. 10a). Topographic profiles following the exhumed unconformity surface along the crests of the folds (Fig. 12) show gradients in the altitude of the folds' crests that are geometrically similar to those shown by the nascent fold (Fig. 9), but which are greatly amplified. The magnitude of crestal uplift is as much as 2 km above local base level along these structures that are 20–50 km long and have noses that plunge at 6–12°. Slope angles for the exposed unconformity surface on the backlimb of these folds were calculated based on a 3-arcsecond DEM of the region. Despite the expected broadening of the slope distributions owing to moderate dissection of the unconformity surface by fluvial channels, most of the slopes on each fold cluster within a few degrees of each other (Fig. 13).

Two of the folds (Xrebet Kara Too and Karacha) show simple along-strike crestal profiles. The largest departures from a smoothly varying profile occur above  $\approx 3500$  m (Fig. 12). We interpret these topographic irregularities to have resulted from glacial erosion and periglacial processes that have incised several hundred metres below the unconformity surface. Despite these topographic departures, the overall smooth profiles are interpreted as a response to growth of a single propagating fault beneath each fold. If this interpretation were correct, it would be expected that the backlimb of the fold would display uniform slope angles along its length. Our field observations on the unconformity surface support this inference. Moreover, slope angles calculated on the backlimbs of the folds (Fig. 13a) clearly show that most of the slopes cluster tightly around the mean slope angle, despite the ongoing dissection of the unconformity surface.

The Gory Baybeiche profile is more complex. Along the 45-km length of the fold, multiple summits and broad exposures of the unconformity are located at  $\approx 3500$  m (Fig. 12). In contrast to the other two folds, the overall altitudinal variation of the fold crest along the Gory Baybeiche structure is smaller. Two major water gaps and several wind gaps interrupt this elongate, rather box-like profile. Satellite images (Fig. 2a) and mapping indicate additional faults with commonly small

displacements (<150 m at the surface) that cut through the backlimb of the fold. We interpret the elongate topographic profile with concordant crestal elevations as resulting from the linkage of several structures whose former terminations are marked by the present water gaps. By analogy with our models (Fig. 3), linkage has led to smoothing of the amplitude gradients along the folds. Additional evidence for linkage of several structures derives from the clear traces of multiple faults that cut the backlimb of the folds and display bow-shaped gradients in the amplitude of offset along these traces. Furthermore, histograms of slope angles (Fig. 13b) show consistent slopes within each individual region of the fold limb that is delimited by a fault, but contrasting slopes between these regions. An alternative explanation would be that the pattern of rock uplift along Gory Baybeiche is simply more box-like with strong displacement gradients at the extremities and very little variation within the intervening part of the structure. This pattern is less compatible with the systematic changes in amplitude displayed by the other folds (Figs 9 and 11), but may represent another mode of fault-fold growth in which abrupt structural discontinuities, such as lateral ramps or tear faults, determine the lateral extent of fold growth (Mueller & Talling, 1997).

### Wind gaps, water gaps and fold propagation

As has been observed in other growing folds (Burbank *et al.*, 1996c; Jackson *et al.*, 1996; Keller *et al.*, 1998), as folds rise and widen, formerly antecedent rivers may be defeated and diverted either around the nose of the fold (Fig. 6) or into a river already traversing the fold, but crossing closer to its propagating nose. When the lateral tips of thrust faults and overlying fold noses propagate toward each other, it would be expected that rivers deflected out of previous antecedent courses would be focused toward the zone of linkage between the two structures (Fig. 12), whereas wind gaps along the fold's crest would mark the former courses of transverse rivers (Jackson *et al.*, 1996).

Along the crest of the Gory Baybeiche fold, there are wind gaps presently at an altitude of  $\approx 3000$ – $3400$  m (Fig. 12). These rivers only succeeded in incising a few hundred metres into the Palaeozoic rocks before they were defeated. Presently, the backlimb of the Baybeiche structure is etched by channels that originate on the unconformity surface and have incised  $\approx 5$ – $20$  m through it (Fig. 2a). The Karacha fold is interrupted near its western terminus by the water gap of the modern At Bashi River, which cuts a gorge several hundred metres deep (Fig. 12). The course of the river turns abruptly westward several kilometres prior to crossing the fold axis. We interpret this pattern to result from deflection of the river during early growth and topographic emergence of the anticline. Given the large discharges of the At Bashi River, it should be able to incise successfully into any rising fold. Rather than incising vertically into

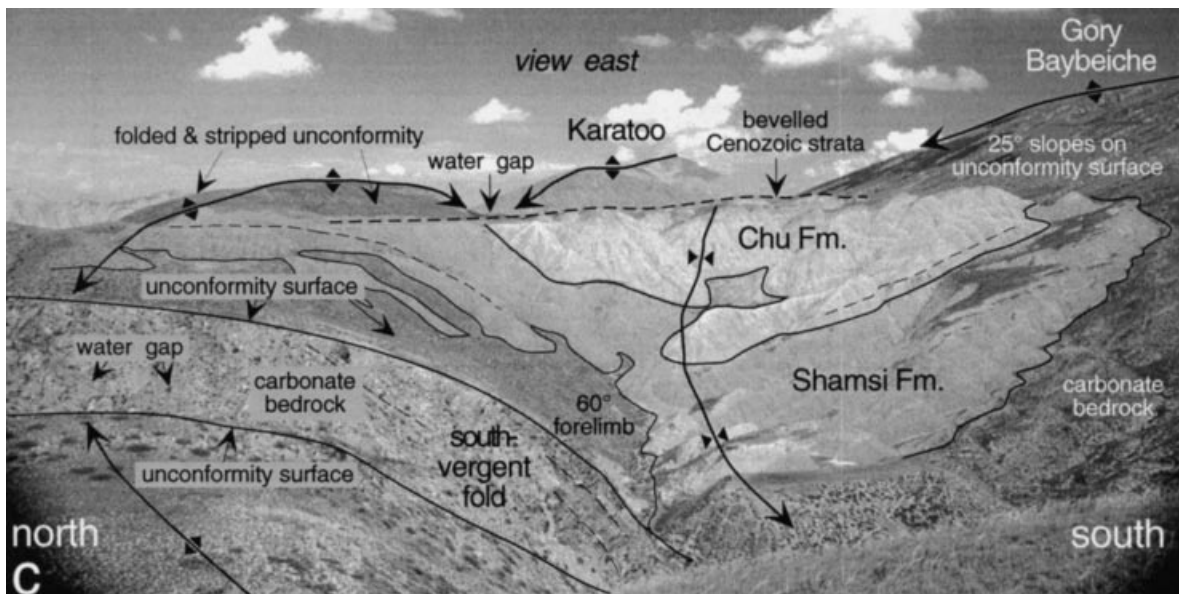
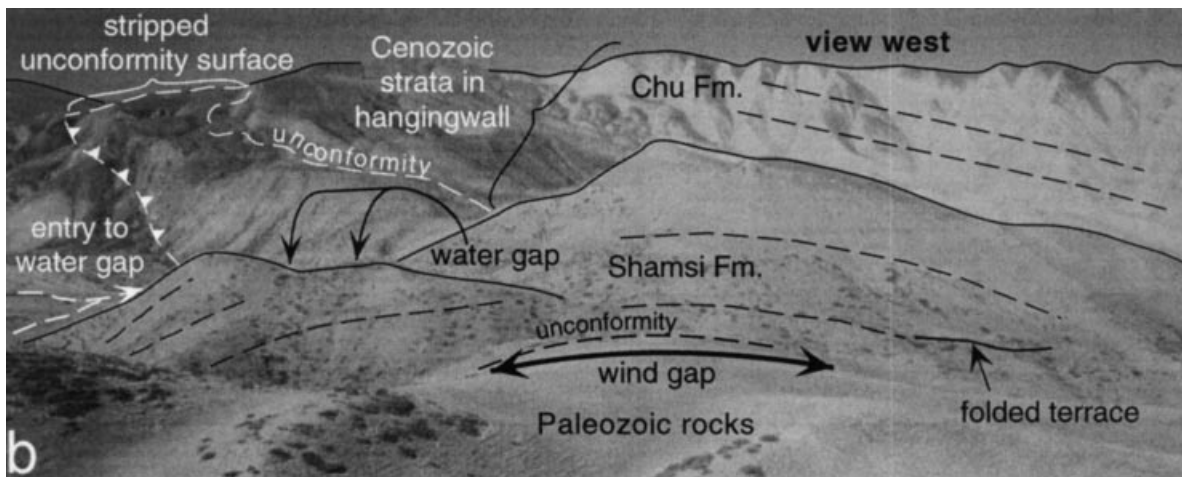
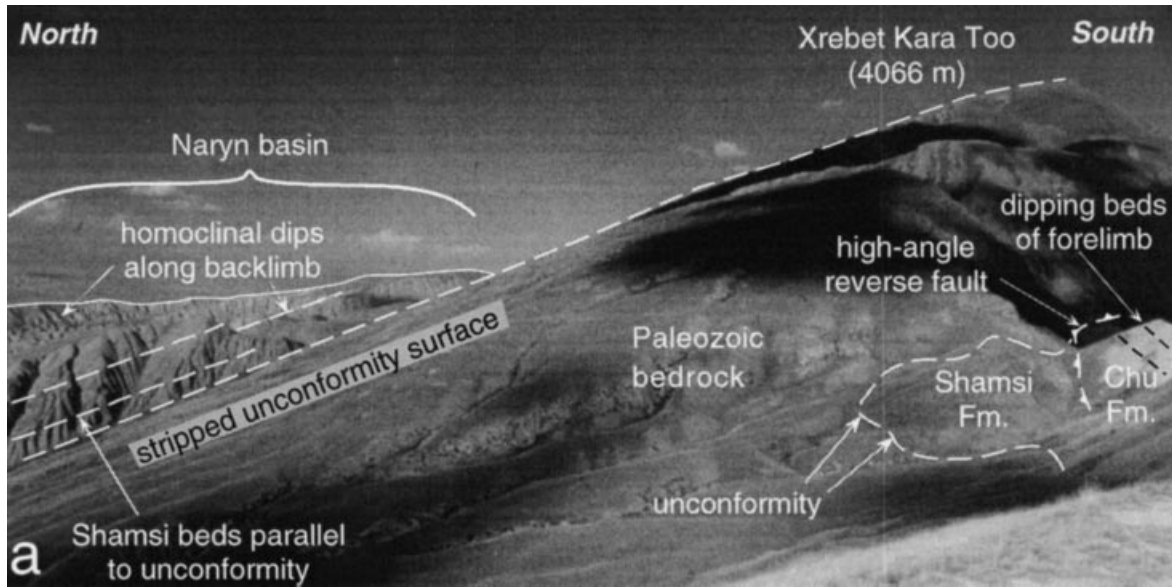
the fold, this apparent deflection suggests that coseismic uplift near the nose of the propagating fold caused westward avulsion into the undeformed floodplain.

Near the western terminus of the Xrebet Kara Too fold, a wind gap (Fig. 10b) provides key evidence concerning interactions of folds and river systems. The wind gap is  $\approx 1.5$  km east of and  $\approx 80$  m above the structural and topographic low point where two folds join and where the present Kara Bulun River crosses the folds via a water gap at or near their juncture. Basal Cenozoic strata exposed adjacent to the wind gap arch across the fold crest (Fig. 10b). South across the Kara Bulun valley from the wind gap, there are alluvial surfaces which project toward the present wind gap and which presently are isolated  $\approx 40$ – $50$  m above the modern valley floor. These alluvial surfaces suggest that a river was flowing through the present wind gap at the time those surfaces were active. The low point of the wind gap coincides with the unconformity surface. Presently exposed at this site, the presence of karstic breccias that developed on the Palaeozoic carbonates as the unconformity was formed indicate very limited dissection of the unconformity surface has occurred. The observations that this low point coincides with the first resistant, i.e. Palaeozoic, bedrock and that the alluvial surfaces across the valley project toward the low point suggest that abandonment of the former water gap occurred at the time these resistant rocks were first encountered (Fig. 6). At that time, the bedrock resistance is interpreted to have exceeded the unit stream power of the traversing river and caused its deflection westward into the water gap where the Kara Bulun River presently flows.

At the Kara Bulun water gap, only the uppermost Palaeozoic bedrock is exposed at the surface (Fig. 11). One might wonder whether this river will soon be defeated, too. This appears unlikely in the short term, because the present water gap is localized in a structural and topographic low between two growing folds: there is no lower position to which the river can be diverted. It is possible that, as the fold amplifies, the river will not be able to keep pace with the rock uplift rate. Rather than resulting in abandonment, however, this may simply cause the upstream catchment to aggrade as the relative elevation of the river bed across the fold crest increases and as the river gradient steepens downstream of the crest.

### Unit stream power through water gaps

Three types of catchment geometries are displayed in the vicinity of the southern Naryn folds (Fig. 8): (1) catchments that extend to the crest, but not across the fold axis; (2) 'hourglass-shaped' catchments that extend through the fold crest and contain water gaps; and (3) catchments on the upstream side of the folds that contain deflected rivers flowing away from or parallel to the folds. Two catchments that feed antecedent rivers transecting Gory Baybeiche (Fig. 14) vary by a factor of  $\approx 4$ – $5$  in



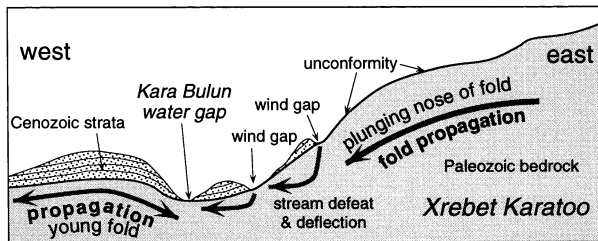


Fig. 11. Structural and geomorphic relationships near the nose of the plunging Xrebet Kara Too fold. Nearly all Cenozoic strata have been stripped off the older Kara Too fold to the east. Two wind gaps, each floored by resistant Palaeozoic bedrock, reflect progressive abandonment of antecedent courses as the fold grew in amplitude and propagated laterally.

their areas and presumably in their discharges, given that they are immediately adjacent to one another so that they should experience similar distributions of precipitation. A steeper river gradient in the smaller catchment, in combination with an observed bankfull width that is  $\approx 40\%$  narrower than in the gorge of the larger catchment, results in a unit stream power that is nearly equal (Fig. 14) between the two catchments. This equality suggests that, as the rivers cut through the water gap and encounter the rising folds, they expend similar energy

on the bed per unit width. This provides a mechanism for maintaining the course of both rivers across the fold, despite their differences in catchment area. Alternatively, this could be conceptualized as the river adjusting its width until its specific stream power is sufficient to drive erosion of its bed at a rate equal to the rock uplift rate.

### Displacement transfer

When the tips of two, oppositely plunging, *en echelon* folds have propagated past each other, our model suggests that shortening can be partitioned between them, such that the total shortening across them remains constant despite variations on an individual structure (Fig. 4). The overlapping and oppositely plunging noses of the Gory Baybeiche and Xrebet Kara Too structures provide a unique opportunity to assess the trade-off in shortening between these folds (Fig. 2). Topographic profiles constructed roughly perpendicular to the fold axes and roughly parallel to the shortening direction (Fig. 15) exhibit characteristics predicted by our model for transfer between folds whose noses overlap: as one fold dies in amplitude, the adjacent one grows (Fig. 4). The amount of shortening could be quantified, if a similar structural level could be followed across both folds. The unconform-

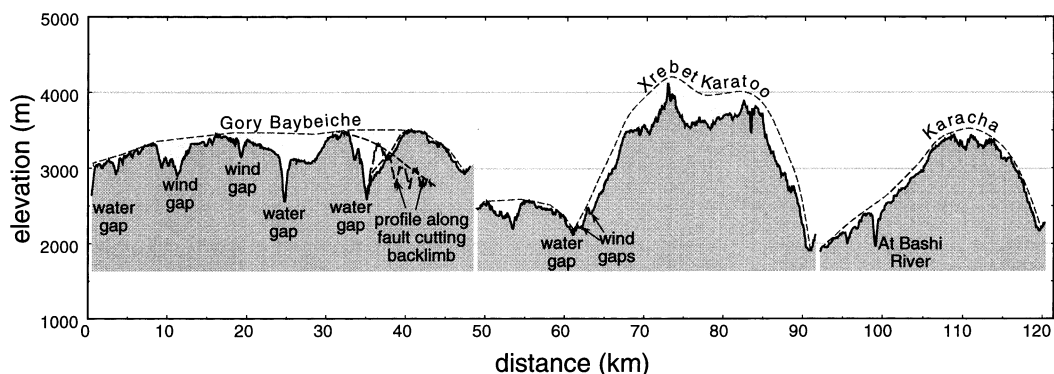
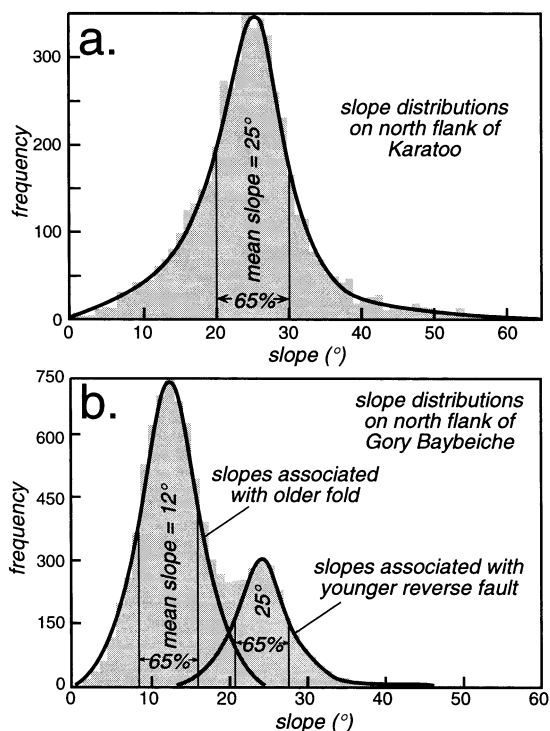


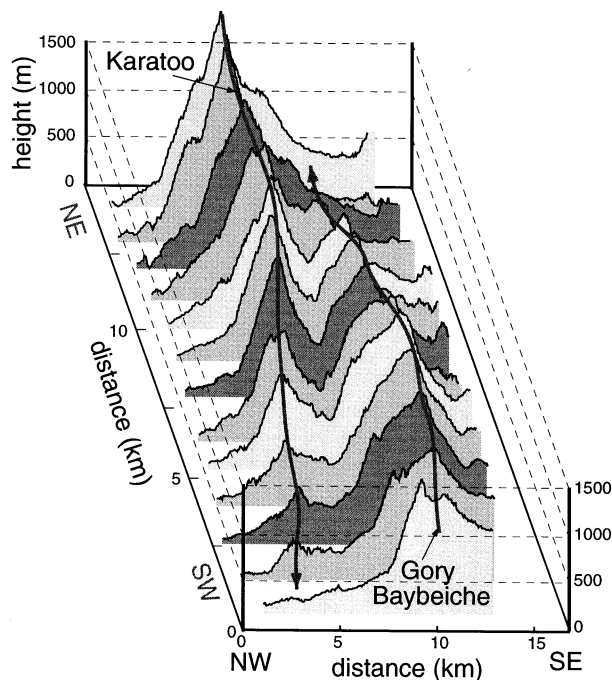
Fig. 12. Longitudinal topographic profiles along the bedrock folds show bow-shaped displacement gradients. Especially near the termini of the folds, the unconformity surface capping the Palaeozoic bedrock has been little modified by erosion. Consequently, the topography mimics the displacement. Prominent water gaps, such as that occupied by the At Bashi River in the Karacha fold, occur near the tips of some structures. Note the wind gaps preserved along several of the folds. The elongate, box-like profile of the Gory Baybeiche structure is interpreted to result from along-strike linkage of several folds. Water gaps through the Gory Baybeiche fold are interpreted to correspond with zones where folds propagating toward each other subsequently linked up. See Fig. 2(b) for location.

Fig. 10. a. Cenozoic strata unconformably overlying Palaeozoic strata along the northern flank of the Xrebet Kara Too fold. Note the parallelism of the Cenozoic bedding and the unconformity, indicating that the unconformity was essentially horizontal during at least the initial stages of Cenozoic deposition. Hence, deformation of that surface post-dates early Cenozoic deposition. Except in a few isolated pockets, Cenozoic strata have been stripped from the folded unconformity surface. High-angle ( $\approx 70^\circ$ ) reverse faults cut the forelimb near the fold crest and juxtapose Cenozoic Shamsi beds with younger Chu strata. b. View down-plunge to the west along the Xrebet Kara Too fold. Basal Cenozoic strata arch across the wind gap (middle ground) and define the crest of the fold. The wind gap is floored by karstic weathering developed along the unconformity surface, suggesting that the wind gap was abandoned at the time that the resistant Palaeozoic strata were encountered by the formerly antecedent river. In the background, a younger fold displays less shortening, a thick mantle of Cenozoic strata on its backlimb and high-angle thrusts cutting its forelimb. c. View east along syncline between the Gory Baybeiche fold and the westward extension of the Kara Too fold (left). The unconformity is folded across the steep forelimb of the Kara Too fold and rises abruptly on the uniformly dipping backlimb of the Gory Baybeiche fold. Cenozoic strata have been eroded down to the altitude of the Palaeozoic strata in the crest of the outer, northerly fold.



**Fig. 13.** Distributions of slope angles on the back limb of the (a) Kara Too and (b) eastern Gory Baybeiche folds. Slope angles are calculated on a 3 × 3 grid (≈ 180 × 180 m) using a 3-arcsecond DEM. Despite dissection of these surfaces, clear mean slope angles are apparent. The double peak on Gory Baybeiche occurs in that part of the fold where a prominent thrust offsets the unconformity surface. The steeper slopes occur on the hangingwall of that thrust which is more rotated than its footwall.

ity surface represents such a level and provides an excellent marker on the backlimbs of these folds. In contrast, on the fold forelimbs, the unconformity may be eroded or buried by talus or by Cenozoic strata, such that it does not coincide with the geomorphic surface. Considering the unconformity surface solely on the backlimbs of the structures, the shortening ranges from 0 to 17% on the individual folds (Fig. 16). When the backlimbs of both structures are considered on transects perpendicular to strike, the total shortening is greatly



**Fig. 15.** Topographic profiles across the oppositely plunging and overlapping termini of the Gory Baybeiche and Xrebet Kara Too folds. The lines of the topographic profiles are orientated roughly perpendicular to the fold axes. Except low on the flanks where Cenozoic strata remain, the topographic surface of both folds is defined primarily by the unconformity surface, such that a similar structural level is being measured in each fold. Note the similarity of the topographic profiles to that predicted when deformation is transferred between two oppositely growing structures (Fig. 4): as one dies, the other grows, and the total shortening remains fairly constant along strike. For location of the cross-sections, see Fig. 2(b).

smoothed across the two folds and averages ≈ 9% (Fig. 16). This is less than the total shortening because it fails to account for folding of the unconformity surface in the buried forelimbs of the folds.

### Structural geometry

Depending on its location, a structure section across the strike of the ranges of the southern Naryn Basin could

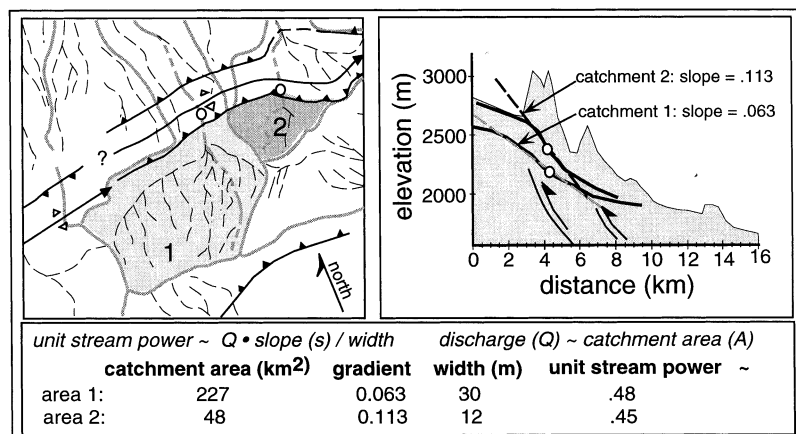


**Fig. 14.** Two catchments crossing Gory Baybeiche fold vary by 400–500% with respect to the catchment area upstream of the water gap and by 250–300% in total stream power. Despite the contrast between the two catchments in the average slope of the river, the specific stream power is calculated to be nearly equivalent between them. See Fig. 8 for location.

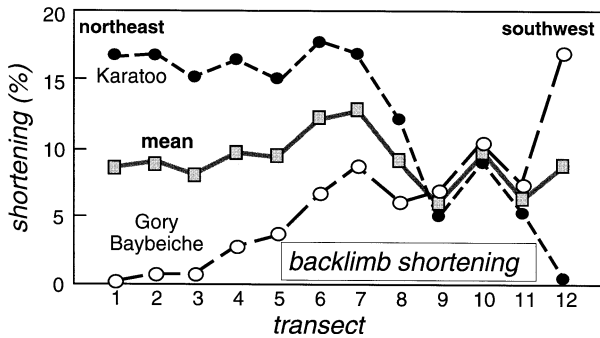


**Fig. 16.** Shortening along the backlimbs of the Kara Too and Gory Baybeiche folds. Shortening is calculated along the exposed unconformity surface and assumes bed length is preserved in the backlimb. Despite large variation along either fold, the mean shortening remains quite constant when both folds are considered in a transect as shown in Fig. 15. For location of transect, see Fig. 2(b).

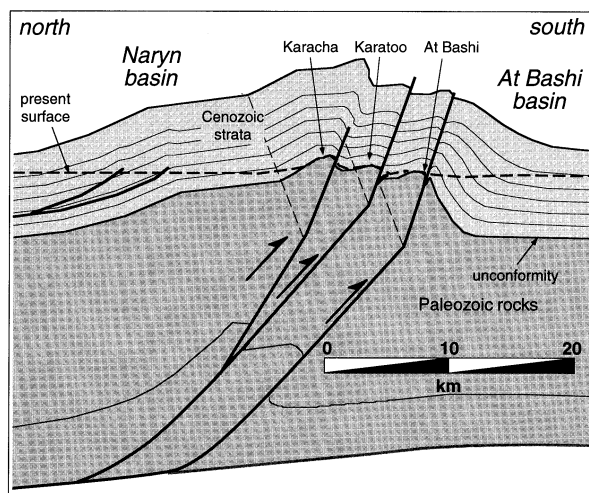


**Fig. 17.** Structural cross-section across the southern Naryn and northern At Bashi basins. The geometry is based on a breakback thrust sequence and utilizes the forward trishear model of Allmendinger (1998) to determine the simplified deformational geometry.

encounter 1–3 large-scale folds or faults involving the Palaeozoic bedrock. A transect located  $\approx 1$ –3 km east of the At Bashi River encompasses three such faulted folds (Figs 2b and 17). Steep reverse faults, typically dipping  $65$ – $85^\circ$  to the NNW, cut the crests or forelimbs of the folds, and commonly offset the unconformity surface by  $< 1$  km. The primary structure in the southern part of the transect is a large, south-vergent fold which we name the At Bashi fold. A continuous panel of Cenozoic strata dipping  $\approx 55$ – $35^\circ$  southward in the forelimb indicates that the structural relief on the fold is approximately 5 km (Fig. 17). Remarkably, despite the structural relief, the At Bashi fold has almost no geomorphic expression. The crest of the anticline is cut by a steep reverse fault that carries the uppermost, slightly overturned Palaeozoic rocks over lower Cenozoic strata in the footwall and has an apparent throw of approximately 0.5 km. At the highest segments of the anticlinal crest, the Palaeozoic

rocks just breach the present-day surface. The backlimb of this fold dips  $20$ – $25^\circ$  to the NNW before being folded into a gentle syncline and cut by a steep ( $\approx 60^\circ$ ) reverse fault that offsets the Palaeozoic rocks and splays into more gently dipping faults ( $< 30^\circ$ ) as it branches into the Cenozoic strata  $\approx 4$  km north of the southern fold. These faults define the southern limit of the Kara Too structure as it dies toward the east. Another 4 km to the north, the Karacha structure is defined by a forelimb that is cut in places by a steep ( $75^\circ$ ) reverse fault (Fig. 13). The Palaeozoic rocks at the crest of the Karacha structure define  $\approx 7$  km of structural relief with respect to the position of the top of the Palaeozoic rocks in the At Bashi basin 15 km to the south (Fig. 17). In the Cenozoic strata to the north of Karacha, dips decrease to  $\approx 5$ – $10^\circ$  across much of the southern Naryn Basin.

Because we lack detailed subsurface data in this area, numerous structural geometries could be compatible with our surface observations. Our structural interpretation is influenced by recent seismic data from elsewhere in the Kyrgyz Tien Shan (Roecker *et al.*, 1993; Ghose *et al.*, 1996; Mellors *et al.*, 1997) which suggest that reverse faults with dips of about  $45^\circ$  often rupture upward through 15–20 km of seismogenic crust. In the study area, our surface observations of reverse faults dipping  $65$ – $80^\circ$  suggest that the deeper faults may steepen within the Palaeozoic rocks near the surface. As Cenozoic strata are encountered by these faults, they become much less steep ( $< 30^\circ$ ) at a few sites. Fold geometries and dips of faults at the surface are consistent with an overall southward vergence in the study area.

Geometric constraints imposed by the relative altitude of the unconformity surface within the ranges suggest that, at the start of growth of the faulted folds described here, the bedrock beneath the Naryn Basin was flexed asymmetrically toward the north. We hypothesize that the load of the ranges bordering the northern basin along the Nikolai Line (Fig. 1) drove this subsidence and imposed an  $\approx 5^\circ$  northward dip on the unconformity surface in the study area. Each of the folds is interpreted to result from a two-stage deformation process. First, a fold developed above the propagating tip of a fault that cut through the seismogenic layer at an angle of  $45$ – $50^\circ$  (Fig. 17). Near the base of the seismogenic crust, the faults become less steep as they merge into a zone of diffuse deformation in the ductile lower crust. Second, as the fault approached the surface, it steepened to the  $65$ – $80^\circ$  dips observed at the surface today. The dip of the backlimbs of the folds results from the steepening of the causative faults within the upper parts of the Palaeozoic rocks.

### Reconstruction of the sequence of deformation

In the absence of reliable chronological control on the timing of each structure, we rely on structural and geomorphic criteria to predict the deformation sequence.

First, we assume that as thrust-related folds develop, they follow a predictable pattern of progressive erosion (Fig. 5), such that degree of preservation of the unconformity surface or the dissection and removal of the Cenozoic strata can be used as a proxy for relative age. Second, if faults offset geomorphic features, they are considered active. Third, the presence or absence of folding of geomorphic markers, such as fluvial terraces, indicates the degree of recent activity on an underlying fold. Fourth, a fold that deflects a river that flows in an undeflected course past the nose of second fold is younger than the second fold. Fifth, in the absence of active faults or deformed geomorphic features, we assume that, once folding begins, the rates of shortening do not vary greatly among individual folds. This assumption would be invalid if, for example, a fold initiated at 2 Ma, but had a growth rate that was 60% slower than a fold that commenced at 1 Ma. At present, we cannot test this assumption. Based on these assumptions, older folds display higher relief, greater incision of Palaeozoic bedrock, more extensive removal of Cenozoic strata, and less continuity of the folded unconformity surface, whereas the younger folds have lower relief, more Cenozoic cover, less Palaeozoic bedrock exposed, less dissection of the unconformity surface and clearer association with deflected rivers.

The reconstructed fold-growth sequence (Fig. 18) indicates that deformation began with growth of the At Bashi fold in the south. The 5 km of structural relief is the largest on any structure in the section. Nonetheless, there is almost no geomorphic expression of this fold, because the Palaeozoic rocks barely reach the geomorphic surface. West of the At Bashi River, a southward-sloping pediment surface and straths which were cut into the Cenozoic strata across the axis of the At Bashi fold are presently isolated 300–600 m above the river. Based on

the position of these surfaces with respect to dated terraces in the Naryn Basin, they are interpreted to be middle Pleistocene in age. More importantly, even though they are cut across the axis of the fold, they are essentially undeformed, indicating that the underlying fold has not been active since the middle Pleistocene (> 130 ka).

The *en echelon* Gory Baybeiche, Kara Too and Karacha structures are interpreted to have developed next. Although the sequencing of development of these three structures is not unequivocal, Kara Too is interpreted as the first to form, based on geomorphic criteria. It is the fold with the greatest relief, greatest dissection of the unconformity surface along its backlimb and most erosion of the Palaeozoic bedrock in its higher, glaciated reaches. Apparently young fault scarps and the recently abandoned wind gap at its west end (Fig. 11) suggest that Kara Too is still propagating westward. Gory Baybeiche and Karacha have many similarities, but Gory Baybeiche is inferred to have formed earlier, because its unconformity surface is slightly more dissected, its elongate crest seems to have formed from linkage of several faults at depth and it is being cut more extensively by younger faults along its backlimb. Like the Xrebet Kara Too and Gory Baybeiche structures, the Karacha fold is almost completely stripped of Cenozoic strata. The At Bashi River has been deflected and then trapped in a water gap along Karacha's eastward propagating nose, whereas the river is undeflected by the Kara Too structure. We interpret this geometry to indicate that the growth of Karacha post-dates that of Kara Too. The small fold to the west of Kara Too (fold 5, Fig. 18) exposes Palaeozoic bedrock in its forelimb, but it has little relief and is mantled in several places by hundreds of metres of Cenozoic strata. The youngest folds to the north and south of the Gory Baybeiche only expose Cenozoic strata, are readily crossed

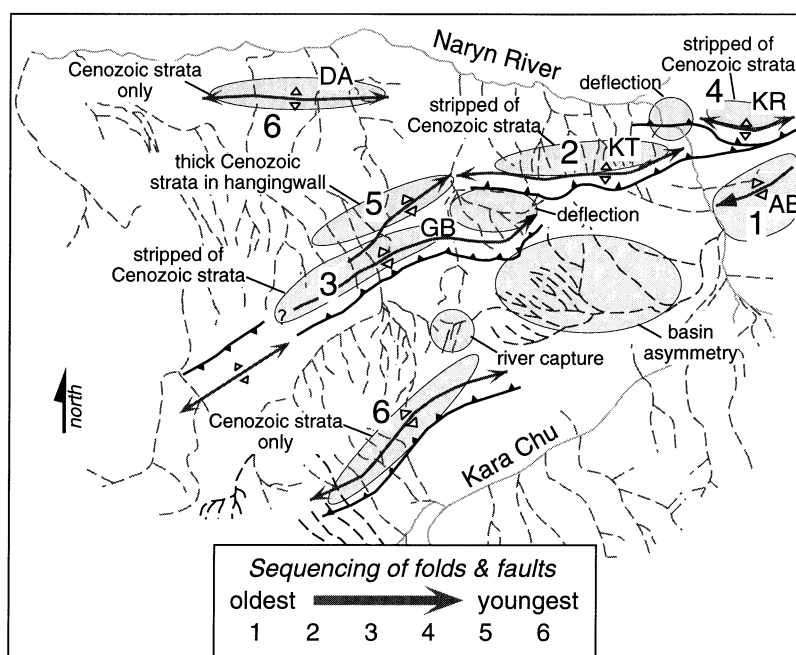


Fig. 18. Reconstructed deformation sequence in the southern Naryn Basin. Criteria for assigning age are described in the text. Examples of basin asymmetry are interpreted to reflect tilting of the bedrock, whereas deflected drainages represent either stream capture or propagating fold noses. AB: At Bashi fold; GB: Gory Baybeiche; KR: Karacha; KT: Kara Too; DA: Dsilan Arik.

by small rivers and have low (<500 m) structural and topographic relief. The fold to the north by Dsilan Arik (Fig. 9a) displays tilted fluvial terraces in the forelimb of the fold, whereas, to the south, there are active faults bounding the south limb of the structure. Examples of river capture, highly asymmetric drainage basins and deflection of drainages (Fig. 18) attest to the dynamic nature of the drainage system in this actively deforming landscape.

## DISCUSSION

Numerous models for the development of thrust-related folds have been recently described (e.g. Suppe, 1983; Jamison, 1987; Medwedeff, 1989; Suppe, 1992; Shaw & Suppe, 1994; Poblet & Hardy, 1995; Wickham, 1995; Vergés *et al.*, 1996; Ford *et al.*, 1997; Poblet *et al.*, 1997; Suppe *et al.*, 1997; Allmendinger, 1998), but most of these consider only two-dimensional cross-sections. Analysis of folds in three dimensions is considerably less common (Philip & Meghraoui, 1983; Medwedeff, 1992; Burbank *et al.*, 1996a; Jackson *et al.*, 1996; Mueller & Talling, 1997; Keller *et al.*, 1998). Growing folds in the southern Naryn Basin of the Kyrgyz Tien Shan provide a natural laboratory in which the evolution of thrust-related folds can be documented. In many areas of the world, growing folds carry only readily erodable Cenozoic strata above local base level, such that the morphology of the fold is often obliterated by erosion soon after being raised above local base level. In the Tien Shan, the presence of resistant Palaeozoic bedrock in the limbs of many folds guarantees their persistence as geomorphic entities, whereas the widespread unconformity that was bevelled across the Palaeozoic rocks provides a robust structural marker for tracking deformation.

During the initial stages of fold growth, slightly indurated Cenozoic strata are raised above local base level and subjected to erosion. The presence of multiple, closely spaced antecedent streams which transect such folds and the highly irregular topography of their emergent limbs attest to the rapid geomorphic modification of the initial structural shape. Although net erosion does not fully balance the rock uplift on these young structures, typically  $\approx 20\text{--}40\%$  of the volume above local base level has been eroded in these low-relief folds (Fig. 9). In contrast, emergent Palaeozoic bedrock on the fold flanks is far more persistent. Efficient erosional stripping of the mantle of Cenozoic strata reveals the folded unconformity surface that faithfully records the geometric shape of the backlimbs of the growing folds. Under the present climate conditions, the exposed unconformity surface is little dissected, even when it is exposed over vertical distances exceeding 1000 m. In such cases, the present topographic surface also defines much of the fold geometry.

Our reconstruction of the sequence of deformation relies on assumptions about the geomorphic evolution of folds in the Tien Shan. Of particular importance are the sequential steps through which surface processes strip the Cenozoic strata off the unconformity surface and

then dissect the Palaeozoic bedrock (Fig. 5). Given the fact that the Cenozoic strata were 5 km thick in this region, an alternative hypothesis can be envisaged: the rivers responded to geometries of folding in the Cenozoic strata far above the unconformity surface and have simply been 'let down' on to the already folded Palaeozoic rocks. In this scenario, the wind and water gaps found today in the Palaeozoic rocks would result simply from competition among drainages on a passive landscape that had already been deformed, rather than a record of the continued growth of these structures. We argue against this interpretation for the following reasons. The slopes of the floors of the wind gaps and of the fluvial terraces within them are sufficiently steep to suggest they have been deformed since abandonment. Even small rivers commonly maintain their courses across folds of Cenozoic strata, so that their deflection appears to result from encounters with the deforming Palaeozoic rocks. The ease of stripping of the Cenozoic strata, in combination with the magnitude of structural relief on the unconformity surface (>7 km), dictates that the Palaeozoic rocks would have emerged as geomorphic entities during deformation, not after it. Seismicity and apparently recent faulting indicates that several of the major bedrock structures are still active.

Several intriguing aspects of these bedrock-involved folds emerge from this study. When the amplitude of the structures is only a few hundred metres, the unconformity surface can be continuously and smoothly traced over the fold crest into both limbs. All of the larger structures have high-angle reverse faults cutting their crests or forelimbs, and it is usually impossible to trace the unconformity within the footwall. Cenozoic strata in the footwall adjacent to the faults typically dip steeply to the south and indicate considerable folding prior to fault propagation to the surface. The backlimbs of each fold display remarkably uniform dips along strike, suggesting that the underlying causative fault maintains a consistent geometry along its length as it propagates laterally and vertically. Where there is more than one fault cutting the fold crest or backlimb, the backlimb dip angles, although highly consistent within the region affected by a given fault, vary strongly between regions associated with different faults (Fig. 13).

It is presently unknown how much limb thinning or thickening occurs in these folds or precisely how the shape and amplitude of the fold is related to displacement on the underlying faults. We suggest that, because the backlimb dips are so laterally persistent, the fault geometry is also laterally persistent. Therefore, even though the fault geometry is not well defined, the relative displacement on these faults can be assessed using the magnitude of deformation of the folds formed above them.

In many fold-and-thrust belts, weak units in former passive margin successions are exploited as detachment horizons (Baker *et al.*, 1988; DeCelles *et al.*, 1995) and, in many cases, the ramps step-up into the foreland-basin fill, such that the young folds involve only synorogenic

strata (Davis *et al.*, 1989; Shaw & Suppe, 1994; Burbank *et al.*, 1996c). This is clearly not the case here, where upper crustal thrusting occurs on ramps that extend many kilometres into the crust (Mellors *et al.*, 1997). Perhaps this is attributable to the Palaeozoic orogenies which created complex bedrock geometries (Burtman, 1975; USSR ANKSaMoG, 1980) in which there are no regionally persistent, rheologically weak layers in a favourable orientation to be exploited by propagating faults. Although the obvious rheological contrast between the Cenozoic strata and the Palaeozoic bedrock could be utilized, it is not the primary detachment surface here.

Simple models and some field studies from other areas (Dawers & Anders, 1995) suggest that the shortening integrated across multiple folds and faults can serve to smooth regional variations in displacement. Although strong variations in fold amplitude and shortening can exist along strike for any given fold, the suite of *en echelon* faulted folds in the southern Naryn Basin provides evidence for a transfer of shortening among adjacent structures that smoothes the overall displacement variations perpendicular to the fold axes. Whereas the tips of these *en echelon* folds are propagating past each other, other folds, such as at Gory Baybeiche, appear to have developed along strike from each other and to have linked up during growth. Such linkage also serves to smooth displacement variations along strike.

Fold-and-thrust belts have traditionally been viewed as migrating systematically away from the hinterland in space and time. It has also been common to envisage that only one thrust was active at a time and that deformation transferred to a new structure only when shortening died or waned on previously active structure. Although recognition of synchronous and out-of-sequence thrusting (Martínez *et al.*, 1988; Morley, 1988; Vergés & Muñoz, 1990; Boyer, 1992; Burbank *et al.*, 1992; DeCelles *et al.*, 1995) and the predictions of critically tapered wedge models (Davis *et al.*, 1983; Dahlen & Suppe, 1988; Dahlen, 1990; Willett, 1992; Willett *et al.*, 1993; Masek & Duncan, 1998) under conditions of nonuniform erosion indicate that thrust sequencing is not uniformly away from the hinterland, the specification of the actual sequence of initiation and motion of thrusts is often difficult to document (Meigs, 1997). Here in the Naryn and At Bashi basins, our reconstruction of the structural evolution suggests that deformation is distributed in space, that multiple structures are active simultaneously and that the initiation of deformation does not migrate systematically across the basin.

The distributed shortening in this small region of the Tien Shan may be representative at the scale of the entire range of the way in which shortening is accommodated. Almost every range front is characterized by thrust fault scarps indicating recent displacement and the Cenozoic strata within many basins are being disrupted by growing structures. The accommodation of convergence between the Tarim Basin and the Kazakh platform by shortening on multiple structures is consistent both with the modern geodetic data and with the recent

seismicity (Roecker *et al.*, 1993; Abdrakhmatov *et al.*, 1996; Ghose *et al.*, 1996, 1998; Mellors *et al.*, 1997). Modern deformation in other fold-and-thrust belts suggests that distributed shortening and coeval displacement may be common phenomena (Seeber *et al.*, 1981; Davis *et al.*, 1989; Hauksson, 1990). Accurate calculation of shortening across these folds, assessment of rates of deformation and their contribution to the geodetically determined rate of 20 mm yr<sup>-1</sup> of shortening across the entire Tien Shan, and better documentation of subsurface fault geometries await further study.

## CONCLUSIONS

We have documented the growth of a suite of thrust-related folds bounding the modern Naryn Basin in the central Tien Shan. Their development partitioned a formerly, much larger depositional basin into two modern subbasins which are dominated by erosion. The geomorphic evolution of these folds is strongly dependent on the particular stratigraphy of the Kyrgyz Tien Shan:  $\approx 5$  km of Cenozoic strata overlying a regionally extensive unconformity cut across rocks deformed in two Palaeozoic orogenies. The contrast in erodability between these two units permits the relative preservation of both the Cenozoic strata and the unconformity surface to be used as proxies for the geomorphic age of a structure. Along the length of a fold, systematic changes in the dissection of the stratigraphy and in fold amplitude correlate with the lateral propagation of the underlying causative faults. Uniform dips of the backlimbs of a given fold suggest remarkably consistent fault geometries along strike. By equating the geomorphic age with a relative geological age, we define a deformational sequence that includes both break-forward and break-back thrusting, rather than a systematic progression of deformation in one direction. Such a sequence is consistent with the broadly distributed seismicity and the presence of multiple, late Pleistocene to Holocene faults within and adjacent to the ranges of the Tien Shan.

## ACKNOWLEDGEMENTS

This research was supported by the NSF Continental Dynamics program (EAR 9614765). We profited from our introduction to the study area by V. Makarov, I. Sadybakasov, A. Korchenkov, O. K. Chediya and P. Molnar, and the support of personnel from the Kyrgyz Institute of Seismology, Kyrgyz Institute of Geology, and IVTRAN, particularly director Y. A. Trapeznikov. Special thanks are extended to A. Mikolaichuk, T. Charimov and Ottar Abdrakhmatov for their extensive assistance and expertise in the field. Field observations, discussions and reviews of this paper by R. Weldon, J. Lavé, S. Thompson, P. Molnar, and C. Rubin contributed immeasurably to this work. We are grateful to Richard Allmendinger for sharing his trishear forward modelling program and to K. Mueller, N. Pinter and

two anonymous reviewers for their incisive critiques of an earlier version of this paper.

## REFERENCES

- ABDRAKHMATOV, K.Y., ALDAZHANOV, S.A., HAGER, B.H., *et al.* (1996) Relatively recent construction of the Tien Shan inferred from GPS measurements of present-day crustal deformation rates. *Nature*, **384**, 450–453.
- ALLMENDINGER, R.W. (1998) Inverse and forward numerical modeling of trishear fault-propagation folds. *Tectonics*, **17**, 640–656.
- ANDERS, M.H. & SCHLEISCHE, R.W. (1994) Overlapping faults, intrabasin highs, and the growth of normal faults. *J. Geol.*, **102**, 165–180.
- BAKER, D.M., LILLIE, R.J., YEATS, R.S., JOHNSON, G.D., YOUSUF, M. & ZAMIN, A.S.H. (1988) Development of the Himalayan thrust zone: Salt Range, Pakistan. *Geology*, **16**, 3–7.
- BOYER, S.E. (1992) Geometric evidence for synchronous thrusting in the southern Alberta and northwest Montana thrust belts. In: *Thrust Tectonics* (Ed. by K.R. McClay), pp. 377. Chapman & Hall, London.
- BOYER, S.E. & ELLIOTT, D. (1982) Thrust systems. *Am. Asso. Petro. Geol. Bull.*, **66**, 1196–1230.
- BROZOVIĆ, N., BURBANK, D.W., FIELDING, E. & MEIGS, A.J. (1995) The spatial and temporal topographic evolution of Wheeler Ridge California: New insights from digital elevation data. *Geol. Soc. Am. Abstr. With Prog.*, **27**, 396.
- BURBANK, D.W., BECK, R.A. & MULDER, T. (1996a) The Himalayan Foreland. In: *Asian Tectonics* (Ed. by Y. An & M. Harrison), pp. 149–188. Cambridge University Press, Cambridge.
- BURBANK, D.W., LELAND, J., FIELDING, E., ANDERSON, R.S., BROZOVIC, N., REID, M.R. & DUNCAN, C. (1996b) Bedrock incision, rock uplift, and threshold hillslopes in the north-western Himalaya. *Nature*, **379**, 505–510.
- BURBANK, D.W., MEIGS, A. & BROZOVIC, N. (1996c) Interactions of growing folds and coeval depositional systems. *Basin Res.*, **8**, 199–223.
- BURBANK, D.W., VERGÉS, J., MUÑOZ, J.A. & BENTHAM, P.A. (1992) Coeval hindward- and forward-imbriating thrusting in the central southern Pyrenees: timing and rates of shortening and deposition. *Geol. Soc. Am. Bull.*, **104**, 1–18.
- BURTMAN, V.S. (1975) Structural geology of Variscan Tien Shan, USSR. *Amer. J. Sci.*, **275-A**, 157–186.
- CARTWRIGHT, J.A., TRUDGILL, B.D. & MANSFIELD, C.S. (1995) Fault growth by segment linkage: an explanation for scatter in maximum displacement and trace length data from the Canyonlands Grabens of SE Utah. *J. Struct. Geol.*, **17**, 1319–1326.
- CHEDIYA, O.K. (1986) *Morphostructure and Neo-tectonics of the Tien Shan*. Academia Nauk Kyrgyz CCP, Frunze.
- CLARK, R.M. & COX, S.J.D. (1996) A modern regression approach to determining fault displacement-length scaling relationships. *J. Struct. Geol.*, **18**, 147–152.
- COWIE, P.A. & SCHOLZ, C.H. (1992a) Displacement-length scaling relationship for faults: data synthesis and discussion. *J. Struct. Geol.*, **14**, 1149–1156.
- COWIE, P.A. & SCHOLZ, C.H. (1992b) Physical explanation for displacement-length relationship of faults using a post-yield fracture mechanics model. *J. Struct. Geol.*, **14**, 1133–1148.
- DAHLEN, F.A. (1990) Critical taper model of fold-and-thrust belts and accretionary wedges. *Ann. Rev. Earth Planet. Sci.*, **18**, 55–99.
- DAHLEN, F.A. & SUPPE, J. (1988) Mechanics, growth, and erosion of mountain belts. In: *Processes in Continental Lithospheric Deformation* (Ed. by S.P.J. Clark, B.C. Burchfiel & J. Suppe), pp. 161–178. Geological Society of America, Denver.
- DAVIS, T.L., NAMSON, J. & YERKES, R.F. (1989) A cross section of the Los Angeles area: seismically active fold and thrust belt, the 1987 Whittier Narrows earthquake, and earthquake hazard. *J. Geophys. Res.*, **94**, 9644–9664.
- DAVIS, D., SUPPE, J. & DAHLEN, F.A. (1983) Mechanics of fold-and-thrust belts and accretionary wedges. *J. Geophys. Res.*, **88**, 1153–1172.
- DAWERS, N.H. & ANDERS, M.H. (1995) Displacement-length scaling and fault linkage. *J. Struct. Geol.*, **17**, 607–614.
- DAWERS, N.H., ANDERS, M.H. & SCHOLZ, C.H. (1993) Growth of normal faults: Displacement-length scaling. *Geology*, **21**, 1107–1110.
- DECELLES, P.G., LAWTON, T.F. & MITRA, G. (1995) Thrust timing, growth of structural culminations, and synorogenic sedimentation in the type Sevier orogenic belt, western United States. *Geology*, **23**, 699–702.
- DIETRICH, W.E., WILSON, C.J., MONTGOMERY, D.R., MCKEAN, J. & BAUER, R. (1992) Erosion thresholds and land surface morphology. *Geology*, **20**, 675–679.
- ELLIOTT, D. (1976) The energy balance and deformation mechanisms of thrust sheets. *Phil. Trans. Royal Soc. Of London*, **283**, 289–312.
- ERSLEV, E.A. (1991) Trishear fault-propagation folding. *Geology*, **19**, 617–620.
- FORD, M., WILLIAMS, E.A., ARTONI, A., VERGÉS, J. & HARDY, S. (1997) Progressive evolution of a fault-related fold pair from growth strata geometries, Sant Llorenç de Morunys, SE Pyrenees. *J. Struct. Geol.*, **19**, 413–441.
- GHOSE, S., HAMBURGER, M.W. & VIRIEUX, J. (1998) Three-dimensional velocity structure and earthquake locations beneath the northern Tien Shan of Kyrgyzstan, central Asia. *J. Geophys. Res.*, **103**, 2725–2748.
- GHOSE, S., MELLORS, R.J., HAMBURGER, M.W., PAVLIS, T.L., KORJENKOV, A.M., OMURALIEV, M. & MAMYROV, E. (1996) The  $M$  (sub  $s$ ) = 7.3 1992 Suusamy, Kyrgyzstan, earthquake in the Tien Shan: 2. Aftershock focal mechanisms and surface deformation. *Bull. Seism. Soc. Am.*, **87**, 23–38.
- HAUKSSON, E. (1990) Earthquakes, faulting, and stress in the Los Angeles basin. *J. Geophys. Res.*, **95**, 15 365–15 394.
- HOMZA, T.X. & WALLACE, W.K. (1995) Geometric and kinematic models for detachment folds with fixed and variable detachment depths. *J. Struct. Geol.*, **17**, 575–588.
- HOWARD, A.D., DIETRICH, W.E. & SEIDL, M.A. (1994) Modeling fluvial erosion on regional to continental scales. *J. Geophys. Res.*, **99**, 13 971–13 913 986.
- JACKSON, J., NORRIS, R. & YOUNGSON, J. (1996) The structural evolution of active fault and fold systems in central Otago, New Zealand: evidence revealed by drainage patterns. *J. Struct. Geol.*, **18**, 217–234.
- JAMISON, W.R. (1987) Geometric analysis of fold development in overthrust terranes. *J. Struct. Geol.*, **9**, 207–219.
- KELLER, E.A., ZEPEDA, R.L., ROCKWELL, T.K., KU, T.L. & DINKLAGE, W.S. (1998) Active tectonics at Wheeler Ridge, southern San Joaquin Valley, California. *Geol. Soc. Am. Bull.*, **110**, 298–310.
- MAKAROV, V.I. (1977) *New Tectonic Structures of the Central*

- Tien Shan (in Russian)*. Order of the Red Banner Geology Institute, Academy of Science, Moscow.
- MARTÍNEZ, A., VERGÉS, J. & MUÑOZ, J.A. (1988) Secuencias de propagación del sistema de cabalgamientos de la terminación oriental del manto del Pedraforca y relación con los conglomerados sinorogénicos. *Acta Geol. Hispánica*, **23**, 119–128.
- MASEK, J. & DUNCAN, C.C. (1998) Minimum-work mountain building. *J. Geophys. Res.*, **103**, 907–918.
- MEDWEDEFF, D.A. (1989) Growth fault-bend folding at southeast Lost Hills, San Joaquin Valley, California. *Am. Assoc. Petrol. Geol. Bull.*, **73** (1), 54–67.
- MEDWEDEFF, D.A. (1992) Geometry and kinematics of an active, laterally propagating wedge thrust, Wheeler Ridge, California. In: *Structural Geology of Fold and Thrust Belts* (Ed. by S. Mitra & G.W. Fisher), pp. 3–28. Johns Hopkins University Press, Baltimore.
- MEGHRAOUI, M., JAEGY, R., LAMMALI, K. & ALBAREDE, F. (1988) Late Holocene earthquake sequences on the El Asnam (Algeria) thrust fault. *Earth Planet. Sci. Lett.*, **90**, 187–203.
- MEIGS, A.J. (1997) Sequential development of selected Pyrenean thrust faults. *J. Struct. Geol.*, **19**, 481–502.
- MELLORS, R.J., VERNOHN, F.L., PAVLIS, G.L., ABERS, G.A., HAMBURGER, M.W., GHOSE, S. & ILLIASOV, B. (1997) The Ms=7.3 1992 Suusamy, Kyrgyzstan earthquake: 1. Constraints on fault geometry and source parameters based on aftershocks and body wave modeling. *Bull. Seismol. Soc. Am.*, **87**, 11–22.
- MICHEL, G.W., REIGBER, C., ANGERMANN, D., KLOTZ, J., CATS-TEAM & GEODYSSEA-TEAM. (1997) Ongoing and recent deformation in Central and SE-Asia. *Eos (Trans. Am. Geophys. Un.)*, **78**, 172.
- MONTGOMERY, D.R. & DIETRICH, W.E. (1992) Channel initiation and the problem of landscape scale. *Science*, **255**, 826–830.
- MORLEY, C.K. (1988) Out-of-sequence thrusts. *Tectonics*, **7** (3), 539–561.
- MUELLER, K. & TALLING, P. (1997) Geomorphic evidence for tear faults accommodating lateral propagation of an active fault-bend fold, Wheeler Ridge, California. *J. Struct. Geol.*, **19**, 397–412.
- OBERLANDER, T.M. (1985) Origin of drainage transverse to structures in orogens. In: *Tectonic Geomorphology: Proc. 15th Annual Binghamton Geomorphology Symposium* (Ed. by M. Morisawa & J.T. Hack), pp. 155–182. Allen and Unwin, Boston.
- OMURALIEV, M. & KORZHENKOV, A. (1995) Morphostructural parameters and stress-deformation state of the medium of seismic zones of the Tien Shan. *Geotectonics*, **29**, 172–179.
- PHILIP, H. & MEGHRAOUI, M. (1983) Structural analysis and interpretation of the surface deformations of the El Asnam earthquake of October 10, 1980. *Tectonics*, **2** (1), 17–49.
- POBLET, J. & HARDY, S. (1995) Reverse modelling of detachment folds in the South Central Pyrenees. *J. Struct. Geol.*, **17**, 1707–1724.
- POBLET, J., McCLAY, K., STORTI, F. & MUÑOZ, J.A. (1997) Geometries of syntectonic sediments associated with single-layer detachment folds. *J. Struct. Geol.*, **19**, 369–381.
- ROECKER, S.W., SABITOVA, T.M., VINNIK, L.P., BURMAKOV, Y.A., GOLVANO, M.I., MAMATKANOVA, R. & MUNIROVA, L. (1993) Three-dimensional elastic wave velocity structure of the western and central Tian Shan. *J. Geophys. Res.*, **98**, 15779–15715 795.
- SADYBAKASOV, I. (1990) *Neotectonics of High Asia (in Russian)*. Nauka, Moscow.
- SCHOLZ, C.H. (1990) *The Mechanics of Earthquakes and Faulting*. Cambridge University Press, Cambridge.
- SCHOLZ, C.G., DAWERS, N.H., YU, J.-Z. & ANDERS, M.H. (1993) Fault growth and fault scaling laws: preliminary results. *J. Geophys. Res.*, **98**, 21951–21921 961.
- SEEBER, L., ARMBRUSTER, J.G. & QUITMEYER, R.C. (1981) Seismicity and continental subduction in the Himalayan arc. In: *Zagros Hindu Kush Himalaya Geodynamic Evolution* (Ed. by H.K. Gupta & F.M. Delaney), pp. 215–242. American Geophysical Union, Washington, DC.
- SHAW, J.H. & SUPPE, J. (1994) Active faulting and growth folding in the eastern Santa Barbara Channel, California. *Geol. Soc. Am. Bull.*, **106**, 607–626.
- SIMPSON, D.W. & ANDERS, M.H. (1992) Tectonics and topography of the western United States – an application of digital mapping. *GSA Today*, **2**, 117–121.
- SLINGERLAND, R., WILLETT, S.D. & HOVIUS, N. (1998) Slope-area scaling as a test of fluvial bedrock erosion laws. *Eos (Trans. Am. Geophys. Un.)*, **79**, 358.
- SUPPE, J. (1983) Geometry and kinematics of fault bend folding. *Am. J. Sci.*, **283**, 648–721.
- SUPPE, J.S., CHOU, G.T. & HOOK, S.C. (1992) Rates of folding and faulting determined from growth strata. In: *Thrust Tectonics* (Ed. by K.R. McClay), pp. 105–122. Chapman & Hall, London.
- SUPPE, J. & MEDWEDEFF, D.A. (1990) Geometry and kinematics of fault-propagation folding. *Ecol. Geol. Helv.*, **83**.
- SUPPE, J., SABAT, F., MUÑOZ, J.A., POBLET, J., ROCA, E. & VERGÉS, J. (1997) Bed-by-bed fold growth by kink-band migration: Sant Llorenç de Morunys, Eastern Pyrenees. *J. Struct. Geol.*, **19**, 443–461.
- SYLVESTER, A.G. (1988) Strike-slip faults. *Geol. Soc. Am. Bull.*, **100**, 1666–1703.
- TALLING, P.J., STEWART, M.D., STARK, C.P., GUPTA, S. & VINCENT, S.J. (1997) Regular spacing of drainage outlets from linear fault-blocks. *Basin Res.*, **9**, 275–302.
- TUCKER, G.E. & SLINGERLAND, R. (1996) Predicting sediment flux from fold and thrust belts. *Basin Res.*, **8**, 329–349.
- TURBIN, L.I., ALEKSANDROVA, N.V. & KONYUKOV, A.G. (1972) The Paleogene and Neogene of northeastern Kirgizia. In: *Geology of the USSR*. Nedra Press, Moscow.
- USSR, A.N.K.S.a.M.o.G. (1980) *Geological map of Kirghiz SSR, scale 1:500 000*. Akad. Nauk Kirghiz SSR and Ministry of Geology, USSR, 6 sheets, scale 1:500 000.
- VERGÉS, J., BURBANK, D.W. & MEIGS, A. (1996) Unfolding: an inverse approach to fold kinematics. *Geology*, **24**, 175–178.
- VERGÉS, J. & MUÑOZ, J.A. (1990) Thrust sequences in the southern central Pyrenees. *Bull. Soc. Géolog. France*, **8**, 265–271.
- WICKHAM, J. (1995) Fault displacement-gradient folds and the structure at Lost Hills, California (U.S.A.). *J. Struct. Geol.*, **17**, 1293–1302.
- WILLETT, S.D. (1992) Dynamic and kinematic growth and change of a Coulomb wedge. In: *Thrust Tectonics* (Ed. by K.R. McClay), pp. 19–32. Chapman & Hall, London.
- WILLETT, S., BEAUMONT, C. & FULLSACK, P. (1993) Mechanical model for the tectonics of doubly vergent compressional orogens. *Geology*, **21**, 371–374.

Received 20 May 1998; revision accepted 20 January 1999